

The Application of Gold Nanorods for Photothermal Therapy of Ovarian Cancer

Chuanzhi LIU¹, Ping GONG¹, Yuping LIANG¹, Zuobin WANG¹, Li WANG^{2*}

¹ School of Life Science and Technology, Changchun University of Science and Technology, 130012, Jilin. China;

² The 208 Hospital of PLA, Changchun, Jilin 130062 China

crossref <http://dx.doi.org/10.5755/j01.ms.26.3.21577>

Received 04 September 2018; accepted 06 January 2019

Photothermal therapy has great significant as a new technology for cancer treatment without side effects. Especially with near-infrared laser as the driving force, which has shown a promising prospect in cancer treatment. However, its application is based on the development of near-infrared laser response of photothermal conversion nanomaterials. Nanogold materials have been studied for a long time as light sensitive materials. The main reason is the surface of the plasmon resonance effect can be adjusted by surface, size and structure, which could make them have excellent performance while absorbing the specific optical wavelength and completing energy conversion. We used the biocompatible gold nano-rods (GNRs) as probes for cancer targeting in order to introduce a progressive synthesis approach in fabricating water-dispersible gold nanorods. These nanorods were prepared by replacing cetyltrimethylammonium bromide with a mixture of 15-polypeptide(15P) molecules. The nano size was estimated about 70–80 nm by electron microscope. The result of dynamic light scattering showed that the cores of the gold nanorods were protected from the outside environment by the 15-polypeptide. Photothermal treatment indicated that 15P-GNRs could stain tumor growth and devote the pivotal steps in promoting cancer cell death with near-infrared laser irradiation. More importantly, these results proved that 15P-GNRs has good bio-compatibility and can be considered as photothermal conversion material for targeting the ovarian tumor.

Keywords: photothermal therapy, gold nanorods, Skov3 cell.

1. INTRODUCTION

The nanocrystal is a particle which is smaller than 100 nanometres, with a special structural and signal-domain crystalline lattice. In the past decade, nanotechnology has developed rapidly and is used widely in biomedical field [1, 2]. Due to the simple preparation, high density, and unique characteristics of optical and electronic properties of nanoparticles, nanotechnology can satisfactorily address concerns related to the development of “multimodal” nanoparticles that can incorporate probes for multiple imaging modalities [3–5]. Metal nanoparticles are the form of nanocomposites, which are especially attractive due to their unique structural and optical properties, including high specific surface areas, high porosities, low densities, and location of plasmon features [6]. Au nanoparticles, also called the gold atom group family (nano atom family) are composed of a plurality of gold atoms with relatively stable aggregates, they exhibit stability, and have a small size effect, quantum effect, and surface effect [7].

Among nano-particles, gold nanorods (GNRs) have attracted much interest as efficient carriers of various diagnostic and therapeutic agents due to their tunable surface plasmon resonance properties, non-toxicity, and biocompatibility [8]. Dr. Lu combined a kind of α -melanocyte stimulating hormone (MSH) molecule (Nle⁴, D-Phe⁷) with Au hollow nano spheres, and then he found

all the cancer cells were dead after the laser irradiation [9]. Reports have recently revealed that the systematic administration of gold nanostructures in animals does not result in any systematic or organ toxicity [10–12]. Exploiting the longitudinal surface plasmon resonance associated with them, GNRs are investigated as the photosensitizer in thermal therapy to kill cancer cell due to the selective heating generated by irradiating them with near-infrared (NIR) light [13, 14]. In 2017, Y.L Wu found that the immune factors of Hemoglobin, red blood cells, neutrophils, lymphocytes and eosinophils could be increased and become much stronger by irradiation with a proper infrared light. It could also make the supply of blood and nutrients to the nerves and muscles partially improved, then make it restored to normal under the infrared light [15]. These attractive features make the GNRs as a new generation of optical probes in cancer-targeting and imaging studies, also in the study of various immunoassays, multiplex imaging of cancer cells, etc [16–18].

Bioactive peptide has been widely used in cancer detection due to the over-expression of its receptors on the surface of neoplastic cells [19]. Although studies focusing on GNRs conjugated with 15P have shown targeted delivery of radio nuclides to cancer cells, few studies have combined the targeting molecules of 15P encapsulated GNRs for cancer detection.

In this paper, the GNRs have shown some incredible results while we combined it with 15P for tumor treatment

* Corresponding author. Tel.: +086-18643020302.
E-mail address: duguchuanzhi@163.com (L. Wang)

in mouse guiding ovarian cancer as the selected solid tumor model. The modified 15P-GNRs were characterized for their targeting, toxicity, cell uptake and tissue absorbing. The photothermal treatment study confirmed the effects of the plasmon resonance of GNRs in the NIR region and the improved targeting efficiency of GNRs at the site of solid tumors. The extensive usage of this novel protocol may open a new avenue for the detection of solid tumors.

2. EXPERIMENTAL SECTION

2.1. Materials

Cetyltrimethylammonium bromide (CTAB), hydrogen tetrachloroaurate (III) trihydrate ($\text{HAuCl}_4 \cdot 3\text{H}_2\text{O}$), Nitrate acid (HNO_3), Hoechst33342, L-ascorbic acid, glutaraldehyde (50 % aqueous solution), sodium borohydride, 15-polypeptide, 10 % RPMI1640 culture medium of fetal bovine serum, 3-(4,5-Dimethylthiazol-2-yl)-2,5-diphenyltetrazolium bromide (MTT), PBS buffer, 4 % paraformaldehyde and Dimethyl sulfoxide solution (DMSO Art.NO.D8370) were purchased from Solarbio.

2.2. Synthesis of bio-compatible GNR and 15P-GNRs

The 15-polypeptide for tumor targeting is made by SHSWHWLPLNRHYAS amino acids [20]. The gold seeds were synthesized using the method described by Liwei Liu in 2011 [21].

According to this method, 15 mL of 30 mmol HAuCl_4 and 300 mL of ultra-pure water were mixed with 12.5 mL of 4.0 mmol HNO_3 solution at 25 °C, 300 mL CTAB and 10 mL ascorbic acid into solution was added gently mixed for 60 s, and the growth solution was finished. While the solution color from orange changed into colorless, the seed solution was added in it. The mixture was stirred overnight at 30 °C.

The GNRs obtained from the previous step were centrifuged again at 7000 rpm for 15 min to eliminate the excess CTAB. Then, 200 μL of the solution containing the GNRs was added to 800 μL of 25 mmol of 15P and mixed with the DMSO solution by a further 48 h of magnetic stirring, leading to the formation of functional 15P-combined with GNRs.

2.3. UV-VIS measurements

The UV-VIS absorbance spectra were acquired at 25 °C. The absorption was measured against water as a reference. The data was collected by Shimadzu UV-3600 spectrophotometer. The absorption spectrum (Fig. 1) is shown before and after the encapsulations and demonstrates the retention of the optical properties.

2.4. Dynamic light scattering assay

Dynamic light scattering was used to monitor the stability of GNRs at the same pH value [22]. The particle size obtained from the DLS images takes into account the polymeric coating and hydration layer surrounding the core

of the GNRs, whereas the images represent only the electron-rich core of the GNRs.

2.5. Cell cytotoxicity assay

SKOV-3 cancer cells were cultured in RPMI1640 medium, 37 °C, 5 % CO_2 cell incubator. When the cell growth on logarithmic phase dispensed into a 96-well plate, each per well has 5×10^3 cells, cultured overnight with RPMI1640 medium plus 10 % FBS. SKOV-3 cells mixed with GNRs and 15P-GNRs at 250 $\mu\text{L}/\text{mg}$ of concentration for 48 h. The cell viability was evaluated by MTT colorimetry assay and the method was referenced to Dr. Liwei Liu's paper on 2011 [23].

2.6. Cell model assay

It has great significance to research the effect of GNRs or 15P-GNRs while combining them with laser irradiation on SKOV-3 cell. There are six groups such as laser radiation, GNRs, GNRs+laser, 15P-GNRs, 15P-GNRs+laser and control groups. The research began by adding 100 μL (0.25 mg/mL) SKOV-3 cells in the 96-well plates for 24 hours, then we added 100 μL (0.25 mg/mL) different concentrations of GNRs or 15P-GNRs before exposed the cell to NIR laser irradiation (25 W/cm^2 , $\lambda = 828 \text{ nm}$, Xi'an Leize BOT808-2000D) for 90 s on each day under the condition of 37 °C, 5 % CO_2 for 48 hours. Finally, added 10 μL MTT (5 mg/ml) into 120 μL DMSO solution after 4 hours and the absorbance was got in 490 nm by microplate reader (Thermo).

GNRs are known to have a large plasmon resonance in the NIR region [23]. 15P-GNRs particles play the part of photosensitizer for improved photo thermal cancer therapy through the efficient localization in the tumor, conducted NIR laser irradiation in an animal model. Female nude mouse 4–5 weeks of age weighing 16–18 g were obtained according to protocols approved by laboratory animal center of Jilin University (NO.201500018550) and were housed 2 per cage, feed by peanut when the experiment finished [24]. SKOV-3 cancer cells were injected oster subcutaneously into the nude mouse ($2.0 \times 10^6/\text{mL}$) about 100 μL . When the tumors grew to approximately 9–10 mm in diameter, 100 μL of the 0.25 mg/ mL 15P-GNRs was injected directly into the tumor areas. The mouse ($n = 3$) were exposed to NIR laser irradiation (55 W/cm^2 , $\lambda = 828 \text{ nm}$) for 90 s on each of six days.

3. RESULTS AND DISCUSSION

3.1. UV-VIS absorbance spectroscopy

Fig. 1 shows that there's a red shift between GNRs and 15P-GNRs. It is apparently due to the change in the dielectric constant of the surface surrounding the GNRs. 15P-GNRs optimum absorption wavelength is about 828 nm.

3.2. Transmission electron microscope images

Fig. 2 a was taken by JEOL model with JEM-2010 microscope while operating at an acceleration voltage of

80 kV. Fig. 2 b was taken by FEI Helios G4 CX dualBeam instrument. Obviously, GNRs were distributed uniformly like some rod shape, with a narrow size about 70–80 nm length, 25 nm width, and covered with smooth surface and clean edge. It was suitable to combine with biological molecules for further assay.

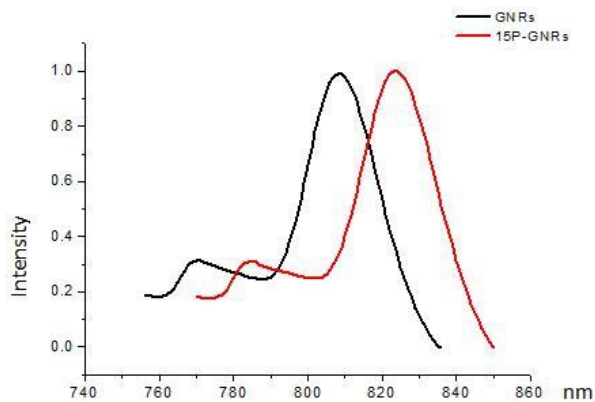


Fig. 1. Absorption spectra show between GNRs and 15P-GNRs

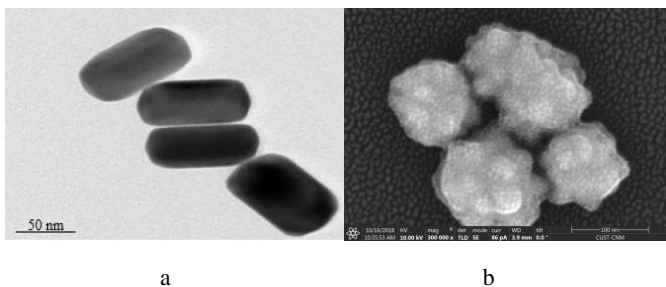


Fig. 2. Scanning electron microscope images of GNRs and 15P-GNRs: a–is for GNRs, the average diameter is about 75 nm; b–is for 15P-GNRs, the average diameter is about 100 nm

3.3. Dynamic light scattering result

According to the results presented in Fig. 3, the encapsulated GNRs are stable, indicating that the cores of the GNRs are protected from the outside environment by the 15-polypeptide.

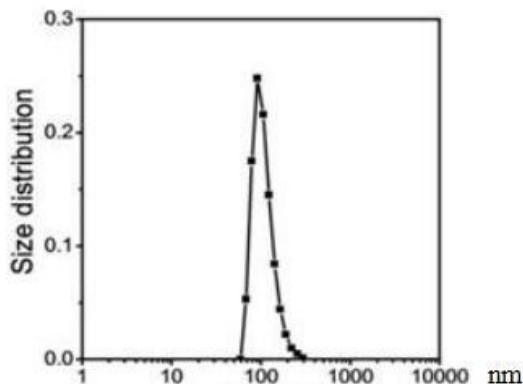


Fig. 3. Test diameters of 15P-GNRs

The GNRs diameter is about 70–80 nm, 15P-GNRs diameter is about 100 nm, so there is about 10–15 nm 15P coating on the GNRs. This could be enhanced the biological compatibility and selective targeting. So it could be used for cancer detection and treatment.

3.4. Cell cytotoxicity result

Fig. 4 shows that the cells' viability value of the GNRs was maintained at 87.6 %, 15P-GNRs was about 90 %. These were indicated less damage to the cells. These particles have negligible in vitro toxicity.

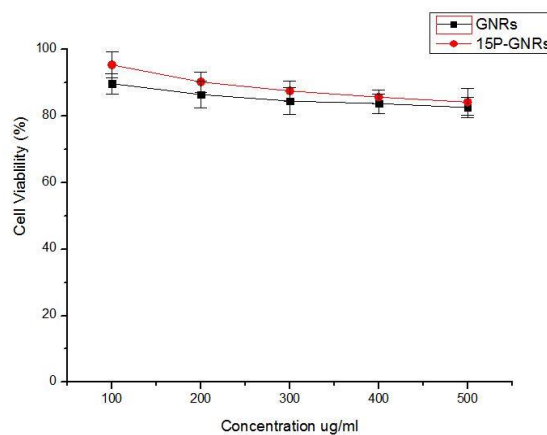


Fig. 4. Viability of SKOV-3 cell at 48 hours and treatment in the presence of GNRs and 15P-GNRs by MTT

3.5. Cell model result

Compared the photothermal behavior of branched GNRs with 15P-GNRs, it is obvious that 15P-GNRs+laser group SKOV-3 cell viability under 20% with control group. Viability of GNRs+laser have just one half (Figure 5). These all remind us that the 15-polypeptide combine with cells, so GNRs have a great photo-thermal efficiency. Data are shown as the means \pm standard error of the means, * $p < 0.05$ and ** $p < 0.01$.

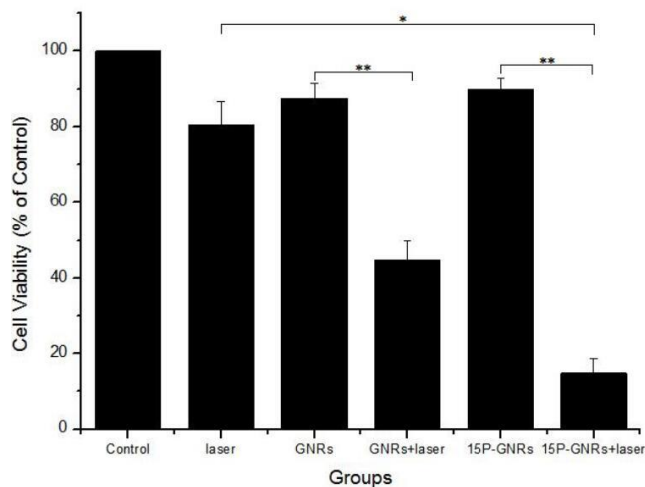


Fig. 5. Viability of SKOV-3 cell under different laser condition

3.5. Animal model

Fig. 6 shows the nude mouse with or without 15P-GNRs under different laser irradiations. The tumor diameter by vernier caliper was got before the treatment and after six days treatment. Fig. 6 a and b show the tumor size (Fig. 6 a) is 9.68 mm before the treatment; the other (Fig. 6 b) is 6.10 mm under laser irradiation conditions with 15P-GNRs injected. Fig. 6 c show the tumor diameter is 8.10 mm. Fig. 6 d is 7.72 mm under laser irradiation without 15P-GNRs injected. The scale bar is 10 mm.

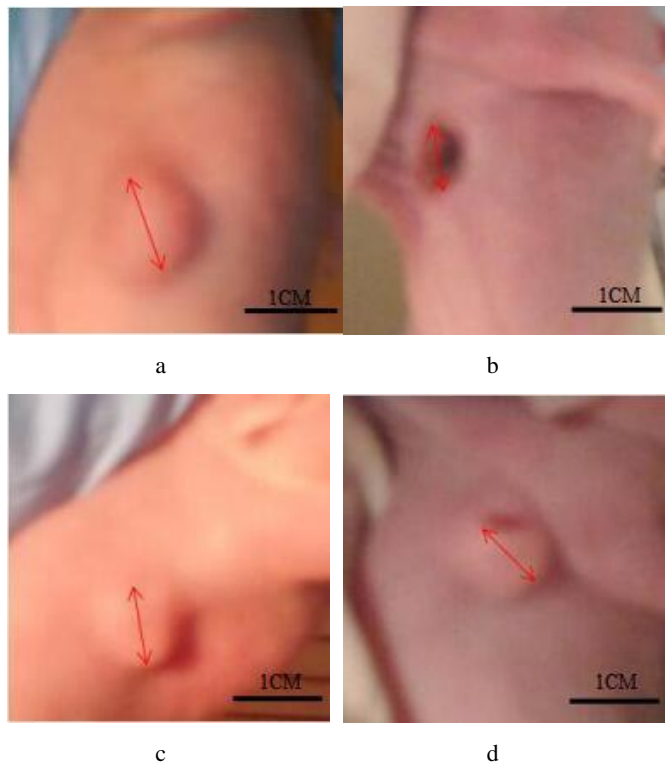


Fig. 6. Tumor size under different treatment: a, c–is the nude mouse before treatment; b–is nude mouse in 15P-GNRs+laser; d–is nude mouse in laser

Table 1. The tumor volume size before (B.T) and after (A.T) treatment

Groups	B.T, cm ³	A.T, cm ³	IR, %
GNRs	0.97 ± 0.07	0.91 ± 0.08	6.18
GNRs+laser	0.87 ± 0.06	0.71 ± 0.06	11.45
15P-GNRs	1.03 ± 0.04	0.86 ± 0.07	16.50
15P-GNRs+laser	0.92 ± 0.05	0.45 ± 0.06	51.09
Laser	0.95 ± 0.06	1.08 ± 0.05	-13.68
Control	0.96 ± 0.07	1.36 ± 0.08	-41.67

According to the data presented in the table the in tumor volume size is different before treatment and after treatment. For example, in 15P-GNRs+laser group before treatment the tumor volume is 0.92 ± 0.05 cm³ as compared injected to the 15P-GNRs treated by laser for 6 days treatment, the tumor volume is 0.45 ± 0.06 cm³. The result indicated that the inhibition rate (IR) of tumor size to other group was relatively higher in 15P-GNRs+laser. What is more 15P-GNRs inhibition rate was just only 16.5 %, this means

15P-GNRs have high photothermal conversion energy. It really effects the tumor cells growth, even kill them. The average tumor size was measured ($V = (\text{length} \times \text{width}^2)/2$) three times for each mouse and there were three nude mouse in one group [25].

Hoechst 33342 staining of the ovarian tumors was performed to determine damage of the tumor. Hoechst 33342 could across the cell membranes and bind to DNA. It is a prominent feature of cell apoptosis in DNA degradation of cell chromosomes. Hoechst 33342 marked DNA in many blue spots, when cells begin to apoptotic. As shown in Fig. 7 with yellow arrows.

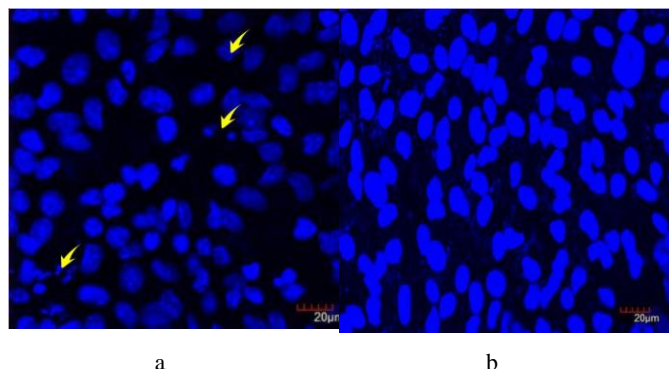


Fig. 7. The tumor cell apoptosis detected by Hoechst 33342: a–arrows show DNA fragments of tumor cell with 15-GNRs+laser; b–apoptotic cell is less than a without treatment

It is obvious that the 15P-GNRs can stain the tumor growth with laser irradiation. The 15P-GNRs exhibited large plasmon resonance in laser irradiation, which led to localized heating that killed the cancer cells. In the study of the relationship between nano-particle and cancer, Dr. Liu [9] found that cancer could chew up nano-particle. As a result, nano-particle would disturb the cell activity, meanwhile, because of the property that nano-particle could change light energy to heat energy, it would also slow down the progress of cancer or even better, kill cancer cells effectively.

4. CONCLUSIONS

This paper has introduced the method for synthesizing 15P-GNRs and the effect of photothermal treatment in tumors. The results suggest that 15P-GNRs show no toxicity in SKOV-3 cell. The cell viability study revealed that 15P-GNRs may serve as a targeting probe for cancer detection and showed excellent physical photothermal characteristics for tumor treatment. 15P could improve the target efficiency of GNRs in tumor diagnosis. Based on these results, 15P-GNRs may be promising as probes for tumor treatment, bio-sensing, drug delivery and other photothermal applications [26].

Acknowledgement

The Youth Fund of School NO.XQNJJ-2017-18 is appreciated.

REFERENCES

1. **He, C.F., Wang, S.H., Yu, Y.J., Shen, H.Y., Zhao, Y., Gao, H.L.** Advances in Biodegradable Nanomaterials for Photothermal Therapy of Cancer; *Advances In Biodegradable Nanomaterials for Photothermal Therapy of Cancer* *Cancer Biology and Medicine* 13 (3) 2017: pp. 299–312. <https://doi.org/10.20892/j.issn.2095-3941.2016.0052>
2. **Shaffer, K.M., Parikh, M.R., Runge, T.M., Perez, S.D., Sakaria, S.S., Subramanian, R.M.** Renal Safety of Intravenous Gadolinium-enhanced Magnetic Resonance Imaging in Patients Awaiting Liver Transplantation *Liver Transplantation* 21 (11) 2015: pp. 247–254. <https://doi.org/10.1002/lt.24118>
3. **Deng, H., Dai, F.Y., Ma, G.G., Zhang, X.** Theranostic Gold Nanomicelles Made from Biocompatible Comb-like Polymers for Thermochemotherapy and Multifunctional Imaging with Rapid Clearance *Advanced Materials* 27 (24) 2015: pp. 36–45. <https://doi.org/10.1002/adma.201501420>
4. **Tang, S., Chen, M., Zheng, N.F.** Sub-10-nm Pd Nanosheets with Renal Clearance for Efficient Near-Infrared Photothermal Cancer Therapy *Small* 10 (15) 2014: pp. 3139–3144. <https://doi.org/10.1002/sml.201303631>
5. **Zhao, P., Zheng, M., Yue, C., Luo, Z., Gong, P., Gao, G.** Improving Drug Accumulation and Photothermal Efficacy in Tumor Depending on Size of ICG Loaded Lipid-polymer Nanoparticles *Biomaterials* 35 (23) 2014: pp. 6037–6045. <https://doi.org/10.1016/j.biomaterials.2014.04.019>
6. **Ding, H., Yong, K.T., Law, W.C., Roy, I., Hu, R., Wu, F.** Noninvasive Tumor Detection in Small Animals Using Novel Functional Pluronic Nanomicelles Conjugated with Anti-mesothelin Antibody *Nanoscale* 3 (4) 2011: pp. 1813–1822. <https://doi.org/10.1039/c1nr00001b>
7. **Martuscello, R.T., Spengler, R.N., Bonoio, A.C., Davidson, B.A., Helinski, J., Ding, H.** Increasing TNF Levels Solely in The Rat Hippocampus Produces Persistent Pain-like Symptoms *Pain* 153 (9) 2012: pp. 1871–1882. <https://doi.org/10.1016/j.pain.2012.05.028>
8. **Masood, R., Roy, I., Zu, S., Hochstim, C., Yong, K.T., Law, W.C.** Gold Nanorod-sphingosine Kinase siRNA Nanocomplexes: A Novel Therapeutic Tool for Potent Radiosensitization of Head and Neck Cancer *Integrative Biology* 4 (2) 2011: pp. 132–141. <https://doi.org/10.1039/c1ib00060h>
9. **Lu, W., Xiong, C., Zhang, G., Huang, Q., Li, C.** Targeted Photothermal Ablation of Murine Melanomas with Melanocyte-stimulating Hormone Analog-conjugated Hollow Gold Nanospheres *Small* 7 (2) 2011: pp. 265–273. <https://doi.org/10.1158/1078-0432.CCR-08-1480>
10. **Seo, S.H., Kim, B.M., Joe, A., Han, H.W., Chen, X., Cheng, Z.** NIR-light-induced Surface-enhanced Raman Scattering for Detection and Photothermal/Photodynamic Therapy of Cancer Cells Using Methylene Blue-embedded Gold Nanorod@SiO₂ Nanocomposites *Biomaterials* 35 (10) 2014: pp. 3309–3315. <https://doi.org/10.1016/j.biomaterials.2013.12.066>
11. **Xiu, L.Y., Fang, M., Zhi, F.D.** Multifunctional Magnetic Nanoparticles for Magnetic Resonance Image-guided Photothermal Therapy for Cancer *Chinese Physics B* 23 (04) 2014: pp. 22–28. <https://doi.org/10.1088/1674-1056/23/4/044301>
12. **Sun, Z.B., Xie, H.H., Tang, S.Y., Yu, X.F.** Ultrasmall Black Phosphorus Quantum Dots: Synthesis and Use as Photothermal Agents *Angewandte Chemie* 127 (39) 2015: pp. 11526–11530. <https://doi.org/10.1002/anie.201506154>
13. **Charan, S., Sanjiv, K., Singh, N., Chen, F.C., Chen, Y.F.** Development of Chitosan Oligosaccharide-Modified Gold Nanorods for in Vivo Targeted Delivery and Noninvasive Imaging by NIR Irradiation *Bioconjugate Chemistry* 23 2012: pp. 2173–2182. <https://doi.org/10.1021/bc3001276>
14. **Mao, B., Chuang, C.H., Lu, F., Sang, L., Zhu, J.** Study of The Partial Ag-to-Zn Cation Exchange in AgInS₂/ZnS Nanocrystals *Physical Chemistry* 117 (1) 2012: pp. 648–656. <https://doi.org/10.1021/jp309202g>
15. **Xu, X., Cheng, F., Ying, Y.B.** Application and Recent Development of Research on Near-infrared Spectroscopy for Meat Quality Evaluation *Spectroscopy and Spectral Analysis* 29 (7) 2009: pp. 1876–1876. [https://doi.org/10.3964/j.issn.1000-0593\(2009\)07-1876-05](https://doi.org/10.3964/j.issn.1000-0593(2009)07-1876-05)
16. **Cheng, L., Liu, J., Gu, X., Gong, H., Shi, X., Liu, T.** PEGylated WS₂ Nanosheets as A Multifunctional Theranostic Agent for in Vivo Dual-Modal CT/Photoacoustic Imaging Guided Photothermal Therapy *Advanced Materials* 26 (12) 2014: pp. 147–155. <https://doi.org/10.1002/adma.201304497>
17. **Chen, Q., Wang, C., Cheng, L., He, W., Cheng, Z., Liu, Z.** Protein Modified Upconversion Nanoparticles for Imaging-guided Combined Photothermal and Photodynamic Therapy *Biomaterials* 35 (9) 2014: pp. 12–23. <https://doi.org/10.1016/j.biomaterials.2013.12.046>
18. **Liang, C., Song, X.J., Chen, Q., Liu, T.** Magnetic Field-enhanced Photothermal Ablation of Tumor Sentinel Lymph Nodes to Inhibit Cancer Metastasis *Small* 11 (37) 2015: pp. 48–56. <https://doi.org/10.1002/sml.201501197>
19. **Yi, X., Yang, K., Liang, C., Zhong, X.Y., Ning, P.** Imaging-Guided Combined Photothermal and Radiotherapy to Treat Subcutaneous and Metastatic Tumors Using Iodine-131-Doped Copper Sulfide Nanoparticles *Advanced Functional Materials* 25 (29) 2015: pp. 4689–4699. <https://doi.org/10.1002/adfm.201502003>
20. **Wang, L., Wang, L., Xu, T., Guo, C., Liu, C., Zhang, H.** Synthesis of 15P-conjugated PPy-modified Gold Nanoparticles and Their Application to Photothermal Therapy of Ovarian Cancer *Chemical Research in Chinese Universities* 30 (6) 2014: pp. 959–964. <https://doi.org/10.1007/s40242-014-4039-5>
21. **Liu, L., Ding, H., Yong, K.T., Roy, I., Law, W.C., Kopwithaya, A.** Application of Gold Nanorods for Plasmonic and Magnetic Imaging of Cancer *Cells Plasmonics* 06 (03) 2011: pp. 105–112. <https://doi.org/10.1007/s11468-010-9175-2>
22. **Ding, H., Yong, K.T., Roy, I., Pudavar, H.E., Law, W.C., Bergey, E.J.** Gold Nanorods Coated with Multilayer

- Polyelectrolyte as Contrast Agents for Multimodal Imaging
Physical Chemistry C 111 (34)
2007: pp. 12552–12557.
<https://doi.org/10.1021/jp0733419>
23. **Liu, L., Law, W.C., Yong, K.T., Roy, I., Ding, H., Erogbogbo, F.** Multimodal Imaging Probes Based on Gd-DOTA Conjugated Quantum Dot Nanomicelles *The Analyst* 136 (8) 2011: pp. 1881–1886.
<https://doi.org/10.1039/C0AN01017K>
24. **Gao, J., Maria, S.P., Huang, H., Wang, S.H.** Synthesis of Different-sized Gold Nanostars for Raman Bioimaging and Photothermal Therapy in Cancer Nano Theranostics *Science China (Chemistry)* 60 (09) 2017: pp. 1219–1229.
<https://doi.org/CNKI:SUN:JBXG.0.2017-09-012>
25. **Naito, S., von Eschenbach, A.C., Giavazzi, R., Fidler, I.J.** Growth and Metastasis of Tumor Cells Isolated from A Human Renal Cell Carcinoma Implanted into Different Organa of Nude Mice *Cancer Research* 46 1986: pp. 4109–4109.
[https://doi.org/10.1016/0304-3835\(86\)90123-0](https://doi.org/10.1016/0304-3835(86)90123-0)
26. **Chou, H.T., Wang, T.P., Lee, C.Y., Tai, N.H., Chang, H.Y.** Photothermal Effects of Multi-walled Carbon Nanotubes on the Viability of BT-474 Cancer Cells *Materials Science and Engineering C* 33 (2) 2013: pp. 989–995.
<https://doi.org/10.1016/j.msec.2012.11.035>